Thermo-Optical, Differential Calorimetric, and Dynamic Viscoelastic Transitions in Poly(2,6-dimethyl-1,4-phenylene oxide) (PPO[1b] Resin) Blends with Poly-*p*-chlorostyrene and with Styrene–*p*- Chlorostyrene Statistical Copolymers[1a]

A. R. Shultz* and B. M. Beach

Polymer Studies Unit, Chemical Laboratory, General Electric Corporate Research and Development, Schenectady, New York 12301. *Received May 30, 1974*

ABSTRACT: Blends of poly(2,6-dimethyl-1,4-phenylene oxide) with poly-*p*-chlorostyrene, styrene–*p*-chlorostyrene statistical copolymers, and polystyrene have been examined by thermo-optical analysis (TOA), differential scanning calorimetry (DSC), and dynamic viscoelastometry (DV). Detection of one or two glass transition regions was used to classify the blends as homogeneous (compatible) or inhomogeneous (incompatible), respectively. PPO resin is compatible with polystyrene and is incompatible with poly-*p*-chlorostyrene. Of the ten styrene–*p*-chlorostyrene statistical copolymers ($M_w \sim 3$–4×10^5) studied, those having the mole fraction of styrene $\bar{N}_s \geq 0.347$ were compatible with PPO resin ($M_w = 0.372 \times 10^5$). Those copolymers having $\bar{N}_s \leq 0.320$ were incompatible with the PPO resin. A copolymer having $\bar{N}_s = 0.334$ appeared to be incompatible with the PPO resin, but the TOA and DSC data were not completely unambiguous. In the five blend systems in which all three experimental techniques were applied, there was agreement as to the homogeneous or inhomogeneous nature of the blends.

Blends of poly(2,6-dimethyl-1,4-phenylene oxide) (PPO resin) with polystyrene have been studied by differential scanning calorimetry (DSC),[2,3] dynamic viscoelastometry (DV),[2] and thermo-optical analysis (TOA).[3b] The viscoelastic behavior of PPO resins has been examined[2,4–6] as well as their calorimetric[7,8] and proton magnetic resonance[9] characteristics. Molecular compatibility of PPO resin with polystyrene at all blend compositions has been proven. Reported instances of inhomogeneity in such blends can be attributed to inefficient mixing methods or to slight segregation of the PPO resin from the blends by crystallization.

The availability of this nearly athermal, probably slightly exothermal, blend of miscible polymers presented a rather rare opportunity. We essayed to gradually change the thermodynamic interaction between the PPO resin and the polystyrene by chemical modification of the latter. Experiments revealed that poly-*p*-chlorostyrene was not miscible with PPO resin. A series of statistical copolymers was prepared to yield copolymer compositions spanning those miscible with PPO resin and those immiscible with PPO resin. The present paper describes the preparation and analysis of some PPO resin blends with polystyrene, poly-*p*-chlorostyrene, and these styrene–*p*-chlorostyrene statistical copolymers.

Experimental Section

Materials. A single PPO resin, having an intrinsic viscosity in chloroform of 0.49 dl/g, M_n = 18,500 by osmometry and M_w = 37,200 by light scattering, was used. The polystyrene (PS) was Lot 4a (Pressure Chemical Co.), an anionically polymerized sample of M = 97,200 and a quoted $M_w/M_n \leq 1.06$.

The poly-*p*-chlorostyrene (PpClS) and the styrene–*p*-chlorostyrene copolymers were prepared by thermal polymerization in degassed, sealed ampoules at 111°. The polymerizates were dissolved in toluene, precipitated into methanol, filtered, and dried in a vacuum oven for 40–72 hr at 80°. Data on the polymerizations and polymers are presented in Table I. Figure 1 displays the composition/conversion relations for nine of the copolymers. These curves were computed[10] from feed and conversion data using relative reactivity ratios $r_1 = 0.797$ and $r_2 = 1.038$ (styrene (1); *p*-chlorostyrene (2)) obtained from an Arrhenius-type interpolation between r_1 and r_2 values obtained[11] at 60 and 131°.

Film Preparation. Polymer mixtures were prepared by weight by dissolving 1 g of mixed polymer powder in 10 ml of toluene and precipitating into 200 ml of methanol in a blender. The resulting fine, fibrous precipitates were filtered, allowed to dry approximately 2 hr in air, and then dried at 80° in a vacuum oven for at least 16 hr. Films ranging in thickness from 0.015 to 0.040 cm were compression molded between aluminum sheets in a hydraulic press. The pressure, applied for 1 min, could not be accurately measured. The films were allowed to cool in air between the sheets to room ambient temperature. The molding temperatures ranged from 180° for the 100% PS, PpClS, and copolymers to 270° for the 100% PPO resin. The blend molding temperatures were elevated above 180° by approximately 1° for each 1 wt % of PPO resin in the blend.

Measurement. Thermo-optical analysis (TOA) data were obtained, as previously described,[3b] by means of an apparatus consisting of a triocular polarizing microscope (Zeiss standard WL) equipped with a hot stage (Mettler FP21) programmed by a control unit (Mettler FP2). Light transmitted through the film sample between crossed (90°) plane polarizer–analyzer plates in the microscope is displayed as a voltage (apparent transmitted light intensity) *vs.* time (temperature) plot on a strip chart recorder (Leeds and Northrup, AZAR, Speedomax). Birefringence is induced in the sample films at room temperature by scribing scratches into their surfaces with a steel stylus. Light is transmitted through the plane polarizer scratched film analyzer system only through the birefringent scratch regions. The microscope aperture, voltage divider, and recorder are initially adjusted to give one-half scale to full-scale voltage readings on the strip chart with the sample stabilized at 60° in the hot stage. The temperature rise controller (10°/min) and the chart drive (⅓ in./min) are simultaneously started. The strip chart record is then essentially a plot of transmitted light intensity *vs.* sample temperature. When polymer segmental motions become sufficiently rapid to relax the stress–strain-induced birefringence in the scratches, the transmitted light intensity rapidly diminishes to a near zero value. The intersection of the tangent to the light intensity–temperature curve at its inflection point with the tangent to the subsequent low slope or zero slope base line locates T_{TOA}, the thermo-optical transition temperature. Normal TOA runs involved scans from 60 to 250°, removal of the sample slide to room ambient, rescratching the film at room temperature, and then a rescan from 60 to 250°. Calibration of the hot stage at +10°/min with naphthalene, adipic acid, and 2-chloroanthraquinone triple points led to 2° subtractions from controller dial readings to give true sample temperatures.

DSC measurements were made on a Perkin-Elmer model DSC-1B differential scanning calorimeter. Sample weights were approximately 10 mg. The heating rate was +20°/min. A nitrogen flow of 0.04 to 0.06 SCFH was passed through the chamber around the sealed aluminum sample and reference containers. Two runs were made from 45 to 280° with sample quenching in between by placing the sample container on a metal surface at room temperature.

The dynamic tensile moduli and phase shift tan δ were measured on film strips of 0.20–0.35 cm width and 0.9–1.2 cm length in a direct reading Dynamic Viscoelastometer Model DDV-II Rheovibron (Toyo Measuring Instruments Co., Ltd.). A single imposed tensile oscillation frequency of 110 Hz was employed. A temperature range from 60 or 80 to 250° (or to sample failure or measuring limit) was scanned at approximately 2.5°/min heating rate. Dynamic force and tan δ were read at about 5° intervals. When com-

Table I
Styrene-*p*-Chlorostyrene Statistical Copolymers

Material	Feed $\bar{N}_s$	% conv	Polymer composition[a] $\bar{N}_s$	$\bar{N}_s$ range	GPC (CH_2Cl_2, 30°)[b] $10^{-5}M_w$	M_w/M_n	M_z/M_w
PS4a	(1.000)		(1.000)		(0.97)		
H	0.469	90	0.454	0.433–0.502	4.05	2.25	1.82
A	0.462	70	0.453	0.439–0.475	3.96	2.20	1.77
G	0.400	99	0.400	0.375–0.458	3.89	2.18	1.79
B	0.387	82	0.377	0.363–0.404	3.88	2.14	1.77
N	0.371	82	0.361	0.347–0.386	2.97	1.89	2.03
M	0.356	82	0.347	0.334–0.371	2.91	1.85	1.93
J	0.343	81	0.334	0.321–0.356	2.97	1.87	1.95
K	0.327	83	0.320	0.307–0.345	2.66	1.93	1.84
C	0.314	73	0.305	0.295–0.320	3.87	2.18	1.87
L	0.286	83	0.279	0.268–0.299	2.82	1.84	1.86
PpClS	0.000	80	0.000		2.85	1.86	1.84

[a] The copolymer compositions, expressed as cumulative $\bar{N}_s$ and $\bar{N}_s$ range, are computed[10] from feed and conversion data assuming $r_1 = 0.797$ and $r_2 = 1.038$ with styrene and *p*-chlorostyrene as monomers 1 and 2, respectively. [b] The gpc column was calibrated with polystyrene samples from Pressure Chemical Co. The copolymer molecular weights were calculated assuming that molecules of equal contour chain length appear at equal gpc elution volume. Therefore, $M = M_{PS}[\bar{N}_S + (138.5/104.1)(1 - \bar{N}_S)]$.

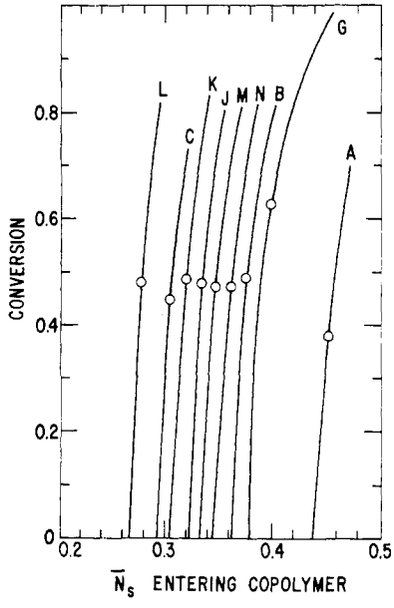

Figure 1. Computed mole fraction of styrene, $\bar{N}_s$, entering copolymer chains as a function of fractional conversion for nine copolymerizations. Open circles represent cumulative $\bar{N}_s$ at termination of the copolymerizations.

puting the elastic moduli, E', corrections were made for the rod and clamp contributions.

Results and Discussion

The principal objects of the present study were to prepare and analyze a systematic series of compatible and incompatible polymer blends and to determine the capabilities of the three experimental methods to detect mobility transitions associated with glass transition regions of these blends. The detection of more than one glass transition as a diagnostic indication of two-phase (or multiphase) structure in the amorphous blends was of special interest. The experimental results will be presented for each of the three analytical methods. A comparison of the findings will then be made to provide an overview of the blend states as revealed by the transition phenomena data.

Thermo-Optical Analytic (TOA) Data. The TOA curves for blends of copolymer A with the PPO resin are shown in Figure 2. Those for blends of PpClS with the PPO resin are shown in Figure 3. A single TOA transition temperature for each copolymer A + PPO resin blend is noted (Figure 2) with the transition temperature increasing monotonically with increasing PPO resin content. Two TOA transition temperatures are noted for each PpClS + PPO resin blend (Figure 3) indicating the two-phase struc-

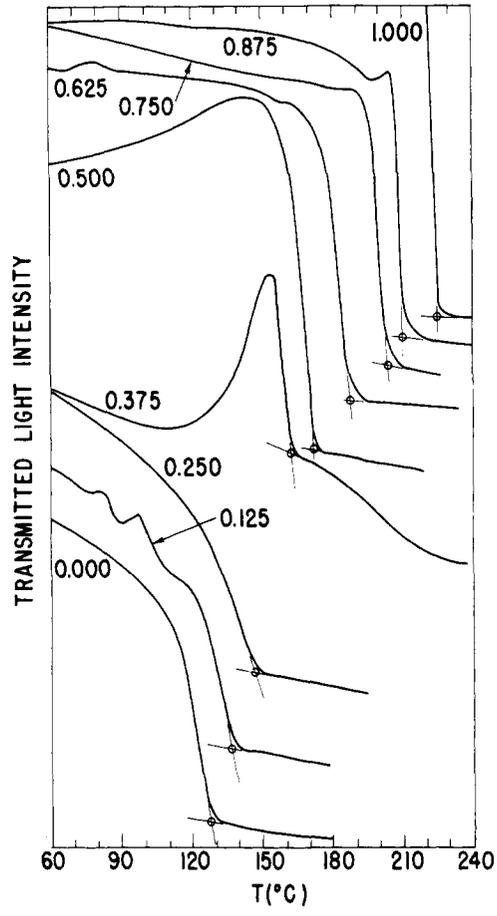

Figure 2. TOA curves for blends of copolymer A with PPO resin. Numbers on the plot represent the weight fraction of PPO resin in each blend.

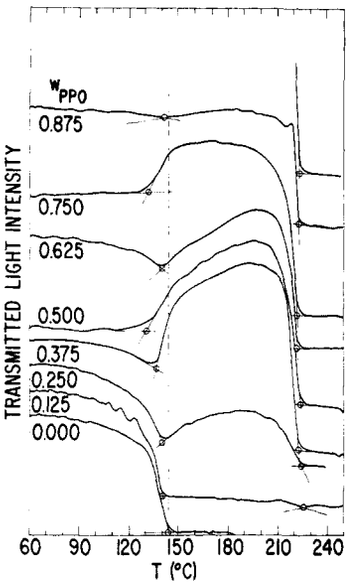

Figure 3. TOA curves for blends of poly-*p*-chlorostyrene with PPO resin. Numbers on the plot represent weight fraction of PPO resin in each blend.

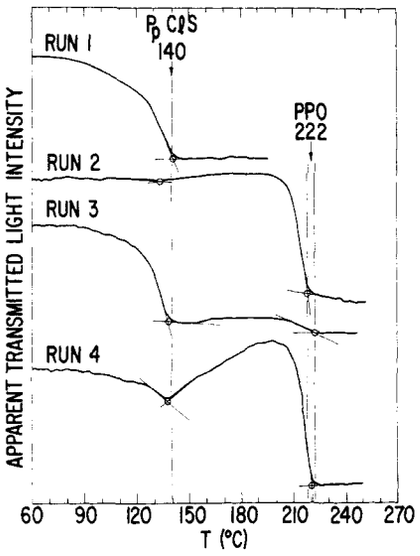

Figure 4. Four successive TOA curves on a single blend film of poly-*p*-chlorostyrene with PPO resin. The weight fraction of PPO resin is 0.625.

ture of the blends. The form of the TOA curves in such heterogeneous blends can vary greatly from one run to the next on a given sample as is shown in Figure 4 for the $w_{PPO} \approx 0.625$ blend of PpClS + PPO resin. However, the two transitions normally remain obvious in each run. Figure 5 presents the thermo-optical transition temperatures of the homogeneous blends of copolymers A, G, and H with PPO resin plotted against the weight fraction of PPO resin. Each point for each blend is an average of two or more transition determinations. The data displayed in Figure 5 are well represented by the least-squares curve (solid line) fitted to the 27 points to give (T_{TOA} in °C)

$$T_{TOA} = 126.8 + 96.5w_{PPO} - 11.0w_{PPO}(1 - w_{PPO}) \quad (1)$$

These data are also fairly well approximated by the curve (broken line) drawn to correspond to

$$1/T_{TOA} = (1 - w_{PPO})/401.2 + w_{PPO}/495.2 \quad (2)$$

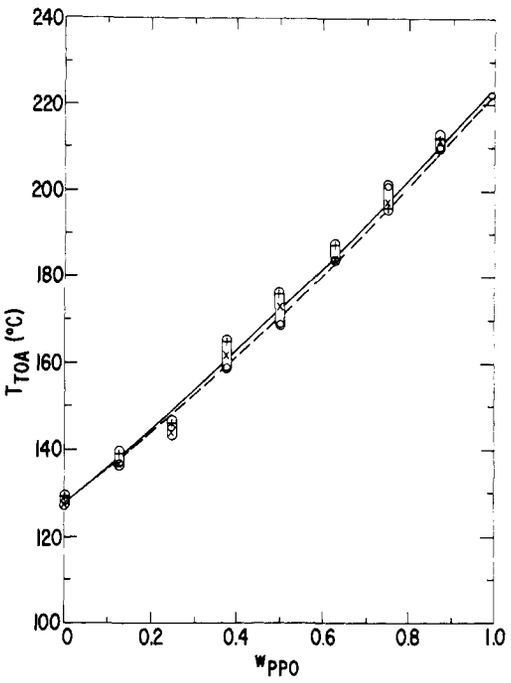

Figure 5. TOA transition temperatures for blends of copolymers H (×), A (○), and G (+) with PPO resin plotted against the weight fraction of PPO resin.

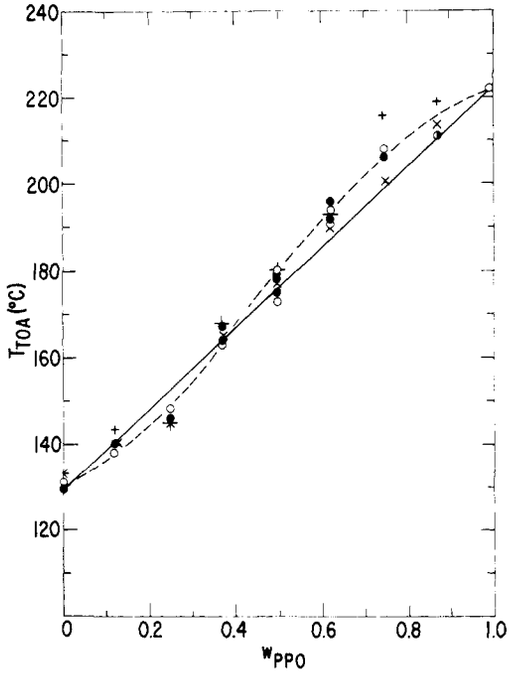

Figure 6. TOA transition temperatures for blends of copolymers B (first run, ○; second or third run, ●), N (×), and M (+) with PPO resin plotted against the weight fraction of PPO resin.

with the denominators of the three terms being T_{TOA} in °K of the blends, of the copolymers, and of the PPO resin, respectively.

The thermo-optical transition temperatures observed for blends of copolymers B, N, and M with PPO resin are shown in Figure 6. The straight line drawn connects 129 and 222°. These data are shown separately from the copolymer A, H, and G blend data because they appear to exhibit a slightly sigmoid character in the T_{TOA} *vs.* w_{PPO} plot. The overall conclusion is that the blends of copolymers B, N, and M with PPO resin are homogeneous but that the

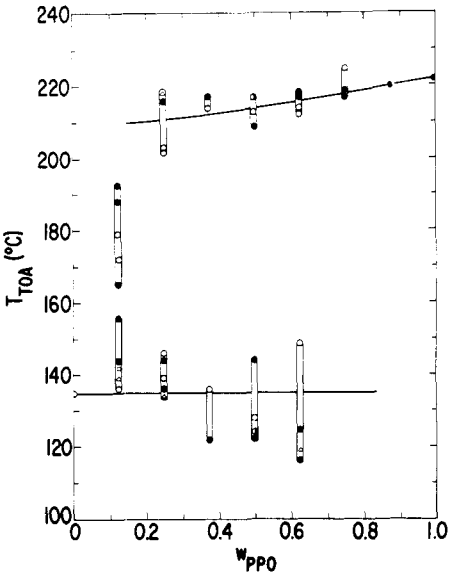

Figure 7. TOA transition temperatures for blends of copolymer C plotted against the weight fraction of PPO resin (first runs, ○; second runs, ●; annealed film runs, □ and △).

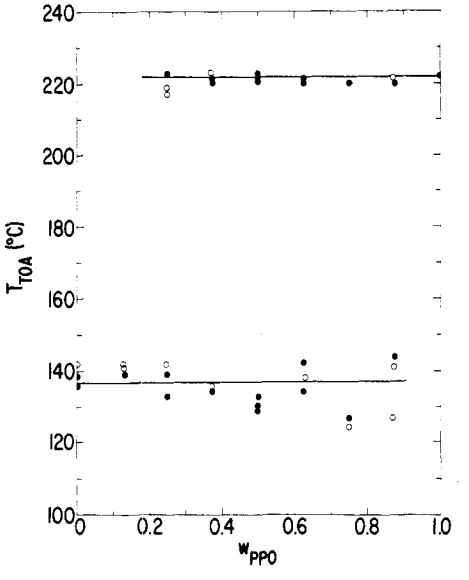

Figure 8. TOA transition temperatures for blends of poly-*p*-chlorostyrene with PPO resin plotted against the weight fraction of PPO resin (first runs, ○; second runs, ●).

majority polymer may be contributing slightly more than its weight fraction share in determining the T_{TOA}.

Figures 7 and 8 are T_{TOA} *vs.* w_{PPO} data representations for the incompatible, two-phase blends of copolymer C + PPO resin and of PpClS + PPO resin, respectively. The TOA measurement readily discerns the mobility transitions in both phases of these two-phase blends. The transitions are very sharp and reproducible for the nearly pure PPO resin phases (Figure 8). A slight lowering of the T_{TOA} of the predominantly PPO resin phase by the presence of copolymer C is indicated in Figure 7. Apparent partial miscibility of the copolymer C and PPO resin in the w_{PPO} = 0.125 blend has not been completely confirmed. The slight downward trend in the lower T_{TOA} *vs.* w_{PPO} lines in both Figures 7 and 8 is principally due to the onset of a rise in transmitted light intensity with temperature increase believed due to increasing form birefringence (*cf.* Figure 3). TOA curves for blends of copolymers L and K with PPO resin also reveal two transition temperatures for the blends

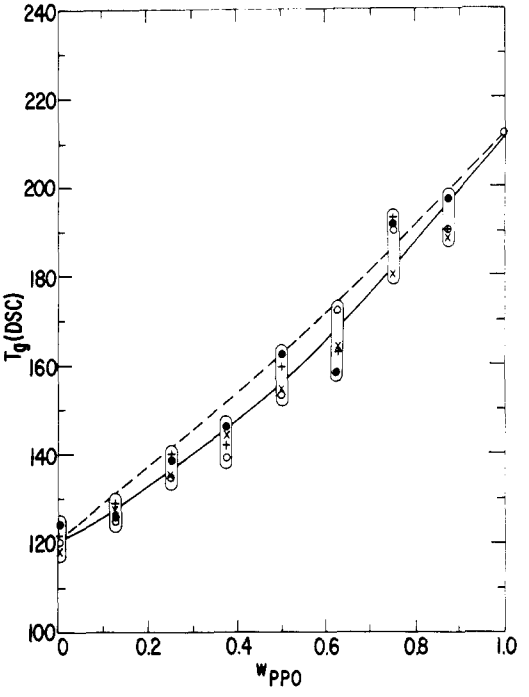

Figure 9. Glass transition temperatures measured by DSC for blends of copolymers H (×), A (○), G (+), and B (●) with PPO resin plotted against the weight fraction of PPO resin.

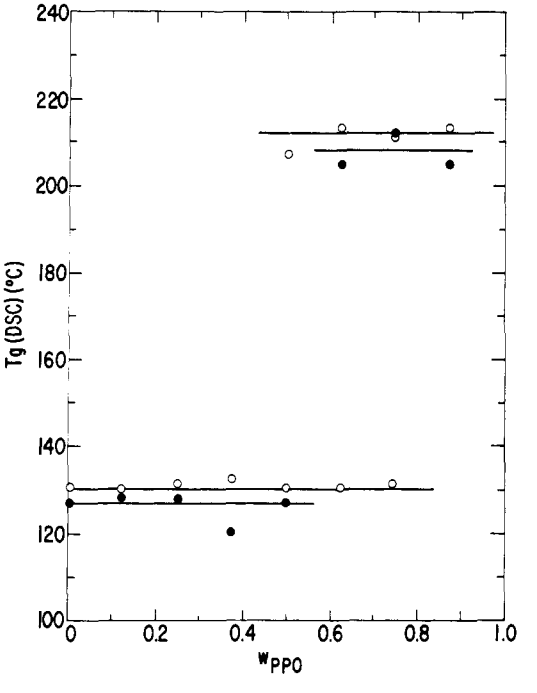

Figure 10. Glass transition temperatures measured by DSC for blends of copolymer C (●) with PPO resin and of poly-*p*-chlorostyrene (○) with PPO resin plotted against the weight fraction of PPO resin.

indicating incompatibility leading to two-phase systems. TOA curves for blends of copolymer J with PPO resin also suggest incompatibility and two transition temperatures. However, when these blends are annealed for 5 min at 220° and then run on TOA single transition temperatures increasing monotonically with PPO resin content are observed. The compatibility or incompatibility of copolymer J with PPO resin is not absolutely determined by TOA.

T_{TOA} for copolymer C is 135° and for PpClS it is approximately 138°. These are appreciably higher than the

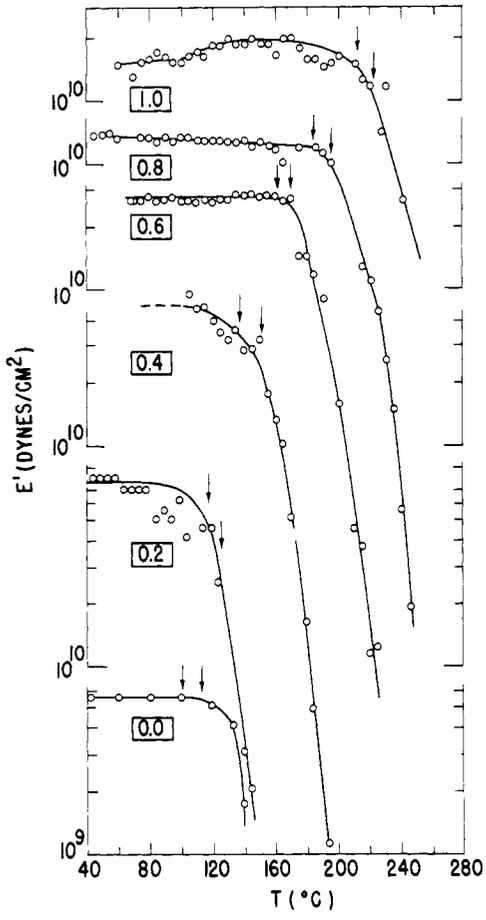

Figure 11. Dynamic tensile elastic moduli *vs.* temperature for polystyrene, for PPO resin, and for blends of polystyrene with PPO resin. Numbers in rectangles represent the weight fraction of PPO resin. For each curve the lower temperature arrow indicates T_g(DSC) and the upper temperature arrow indicates T_{TOA} (*cf.* ref 3).

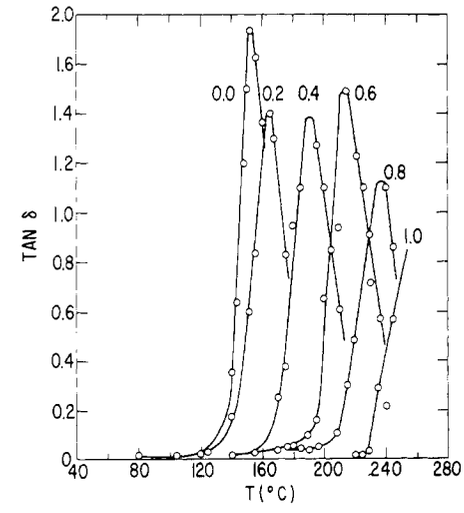

Figure 12. Loss tangents *vs.* temperature. *Cf.* Figure 11 legend. The maxima lie at 152, 165, 190, 214, and 236° for the materials having weight fraction PPO resin 0.0, 0.2, 0.4, 0.6, and 0.8, respectively.

$T_{TOA} \simeq 130°$ for copolymer B and 128–129° for copolymers A, H, and G. All the PpClS + PPO resin blend films possess haze visible to the unaided eye. Copolymer C + PPO resin blend films having w_{PPO} = 0.375, 0.500, 0.625, and 0.750 also appear hazy. However, the copolymer C +

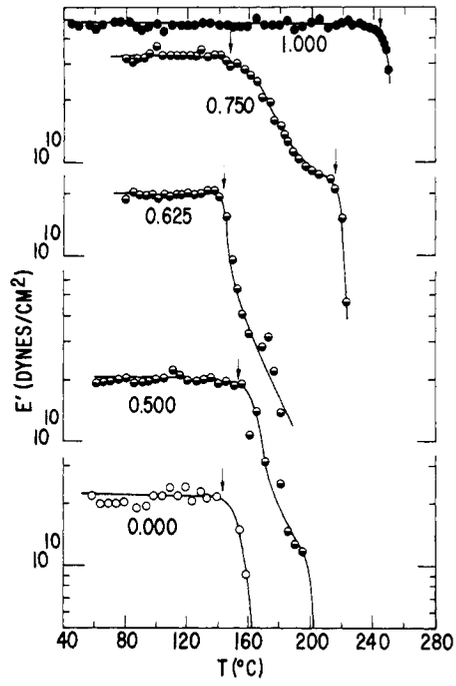

Figure 13. Dynamic tensile elastic moduli *vs.* temperature for poly-*p*-chlorostyrene, for PPO resin, and for blends of poly-*p*-chlorostyrene with PPO resin. Numbers represent the weight fraction of PPO resin. Arrows indicate the approximate temperatures of modulus transition onset.

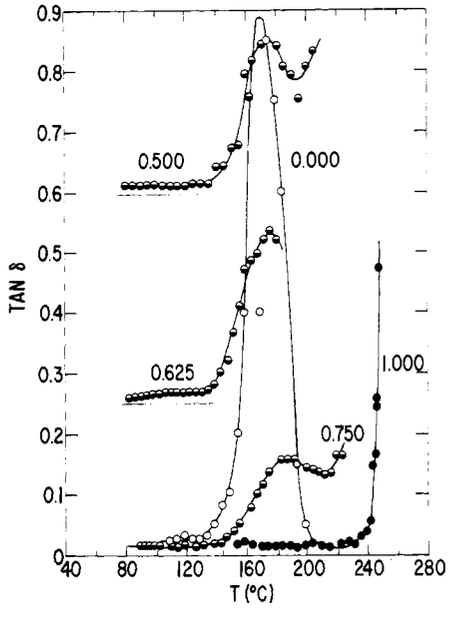

Figure 14. Loss tangents *vs.* temperature. *Cf.* Figure 13 legend. Note the base-line shifts for w_{PPO} = 0.500 and 0.625.

PPO resin blend films having w_{PPO} = 0.125, 0.250, and 0.875 would be judged "clear" by most observers.

Differential Scanning Calorimetric (DSC) Data. The glass transition temperatures according to DSC of the PPO resin blends with copolymers A, H, G, and B are shown in Figure 9. T_g(DSC) for pure copolymers A, H, G, and B were found to be 120, (118), 121, and 124°. The T_g(DSC) values shown in Figure 9 each represent the average of two determinations. The DSC data for these various homogeneous blends exhibit such scatter that, despite the somewhat different values of T_g for the pure copolymers, a single T_g(DSC) *vs.* w_{PPO} relation for the entire set is as satisfactory as any. Least-squares fitting of the 36 averaged

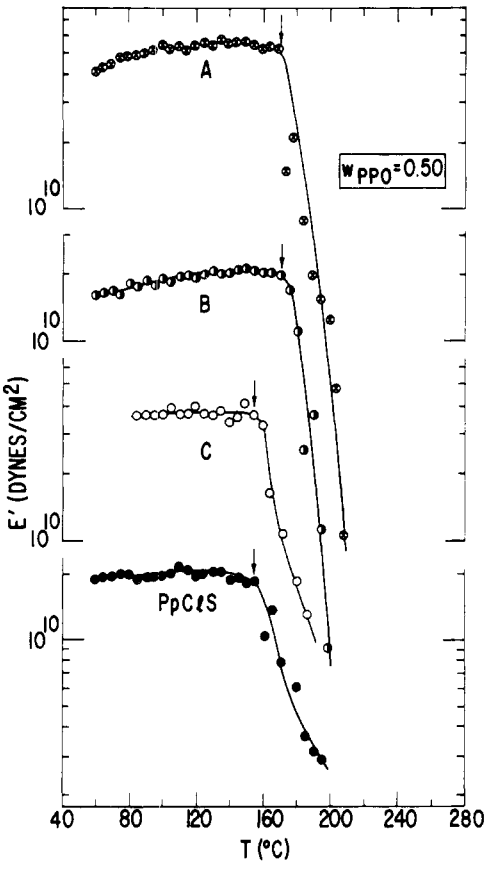

Figure 15. Dynamic tensile elastic moduli *vs.* temperature for blends of PPO resin with copolymers A, B, and C, and with poly-*p*-chlorostyrene. The PPO resin weight fraction is 0.50.

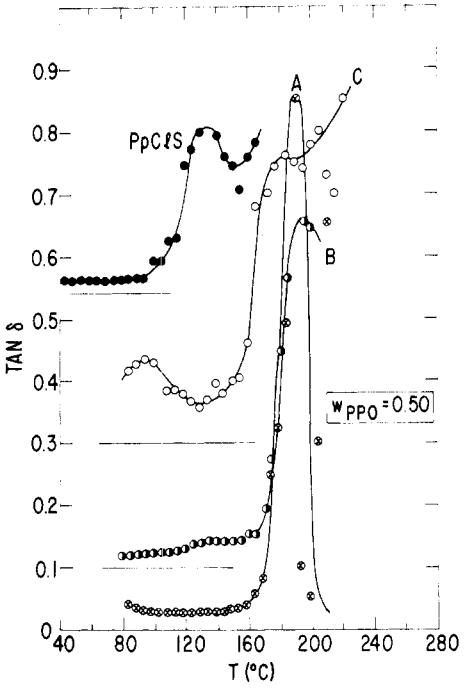

Figure 16. Loss tangents *vs.* temperature. *Cf.* Figure 15 legend. The PPO resin weight fraction is 0.50. Note the base-line shifts.

data points, including four data for pure PPO resin, yields (T in °C)

$$T_g(\text{DSC}) = 120.0 + 91.5w_{\text{PPO}} - 40.5w_{\text{PPO}}(1 - w_{\text{PPO}}) \quad (3)$$

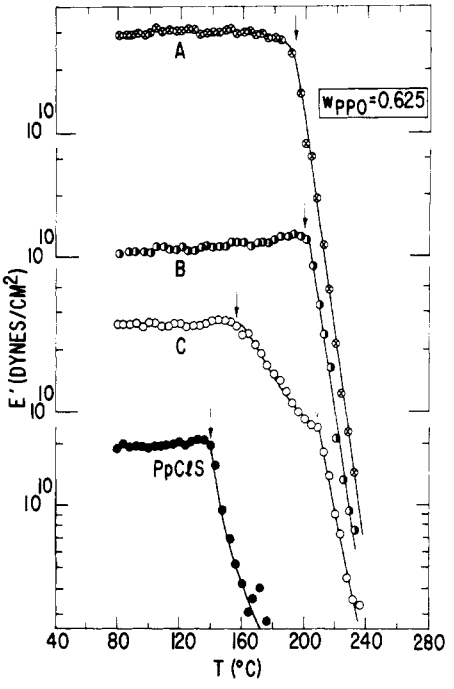

Figure 17. Dynamic tensile elastic moduli *vs.* temperature for blends of PPO resin with copolymers A, B, and C and with poly-*p*-chlorostyrene. The PPO resin weight fraction is 0.625.

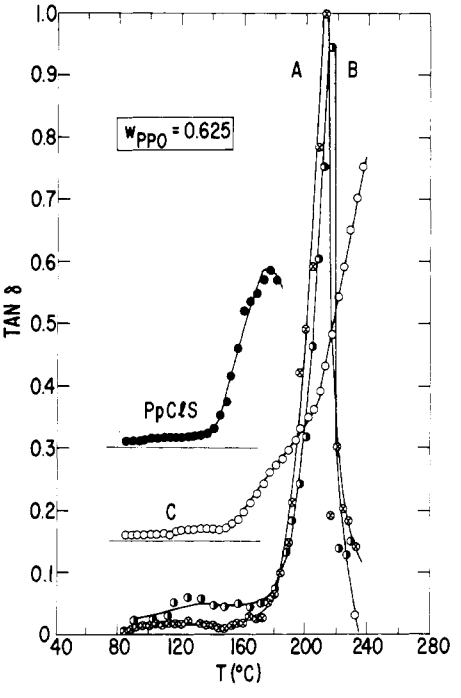

Figure 18. Loss tangents *vs.* temperature. *Cf.* Figure 17 legend. The PPO weight fraction is 0.625. Note the base-line shifts.

The solid curve in Figure 9 represents eq 3.

The broken line curve in Figure 9 is drawn according to the relation

$$1/T_g(\text{DSC}) = (1 - w_{\text{PPO}})/394.2 + w_{\text{PPO}}/485.2 \quad (4)$$

where T_g(DSC) is in °K. Although the T_g(DSC) data are less reproducible than one would wish, Figure 9 does indicate that the blends of PPO resin with copolymers A, H, G, and B are homogeneous as judged by a single T_g(DSC) intermediate between the transitions of the pure components

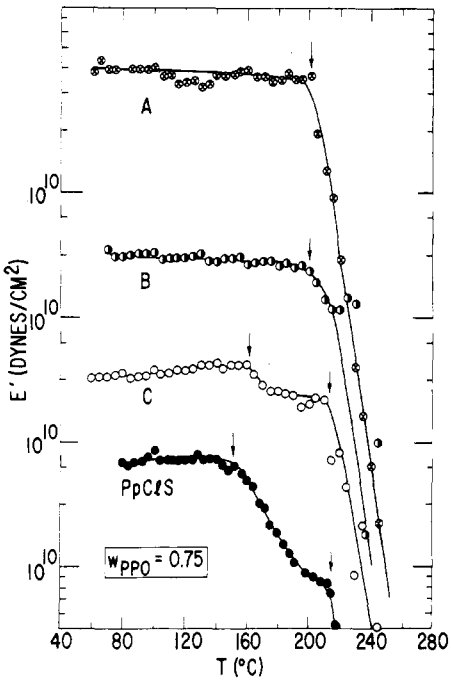

Figure 19. Dynamic tensile elastic moduli *vs.* temperature for blends of PPO resin with copolymers A, B, and C and with poly-*p*-chlorostyrene. The PPO resin weight fraction is 0.75.

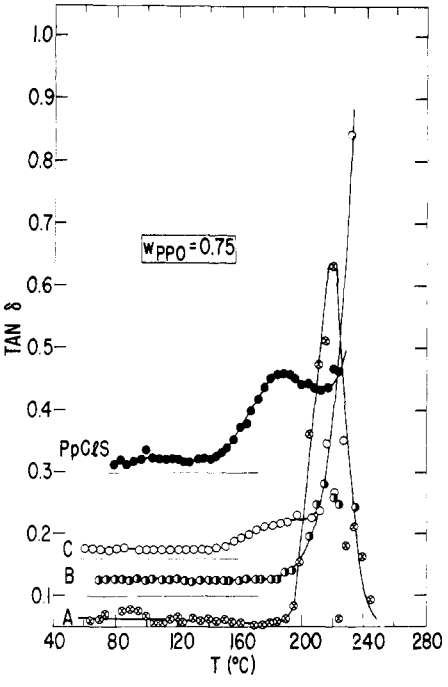

Figure 20. Loss tangents *vs.* temperature. *Cf.* Figure 19 legend. The PPO resin weight fraction is 0.75. Note the base-line shifts.

comprising the blends. Blends of PPO resin with copolymers N and M also yield single T_g(DSC) values indicating compatibility.

The T_g(DSC) of the copolymer C + PPO resin and PpClS + PPO resin blend films are depicted in Figure 10. T_g(DSC) corresponding to essentially pure individual polymer phases are noted. The T_g(DSC) for copolymer C, PpClS, and PPO resin were measured as 127, 130, and 212°, respectively. Under our operating conditions we detected only the T_g(DSC) of the lower transition for $w_{PPO} \leq 0.375$. T_g(DSC) were detected for both the PpClS phase and the PPO resin phase at w_{PPO} = 0.50, 0.625, and 0.750,

Table II
Compatibility (+) or Incompatibility (−) of Copolymers with PPO Resin as Judged by One or Two Transitions, Respectively

Material	$\bar{N}_s$	Measurement		
		TOA	DSC	DV
PS4a	1.000	+	+	+
H	0.454		+	
A	0.453	+	+	+
G	0.400	+	+	
B	0.377	+	+	+
N	0.361	+	+	
M	0.347	+	+	
J	0.334	−?	−?	
K	0.320	−	−	
C	0.305	−	−	−
L	0.279	−	−	
PpClS	0.000	−	−	−

while beyond w_{PPO} = 0.50 only the T_g(DSC) of the PPO resin phase was detected in the copolymer C blends. It is believed that more sensitive DSC measurements might detect the T_g transition of the minority component phase in each of the blends. Copolymers L, K, and J were found to give blends with PPO resin which exhibited T_g(DSC) for the majority component phase, demonstrating incompatibility in the blends. The blends of copolymer K + PPO resin and copolymer J + PPO resin showed some elevation of the lower T_g(DSC) by PPO resin and lowering of the upper T_g(DSC) by the copolymer. Incorporation of some of the minority component polymer into the majority component phase was indicated.

Dynamic Viscoelastic (DV) Data. Figures 11 through 20 display the dynamic tensile elastic moduli, E', and the loss tangents, tan δ, at 110 Hz frequency as functions of temperature for PPO resin blends with polystyrene, PpClS, and the copolymers C, B, and A.

The polystyrene + PPO resin blends (Figures 11 and 12) exhibit single E' decrease regions and single tan δ peaks located at temperatures increasing monotonically with increasing PPO resin content. These data indicate homogeneous blends. On the other hand, the PpClS + PPO resin blends (Figures 13 and 14) exhibit two E' decrease regions and tan δ peaks corresponding in temperature to the tan δ peak temperature of the essentially pure PpClS phase. Beyond these initial peaks the tan δ values again rise. The second peaks in tan δ, corresponding to the transition of the essentially pure PPO resin phase, are not reached due to sample failure under the continuously applied tensile force. The peak in tan δ of the pure PPO resin (Figure 14) lies above 250° and was not reached due to the limitation of measurements to 250° and below.

Figures 15, 17, and 19 display the single E' drop regions of the homogeneous copolymer A + PPO resin and copolymer B + PPO resin blends and the double E' drop regions of the inhomogeneous PpClS + PPO resin and copolymer C + PPO resin blends. The tan δ *vs.* T curves (Figures 16, 18, and 20) correspondingly exhibit single peaks increasing monotonically in temperature with increasing PPO resin content for the copolymer A + PPO resin and copolymer B + PPO resin blends. With the exception of the erratic tan δ data at w_{PPO} = 0.500 for copolymer C + PPO resin, the inhomogeneous copolymer C + PPO resin blends exhibit a shoulder in the tan δ *vs.* T curves at a temperature corresponding closely to the tan δ peak of the PpClS + PPO

resin blends followed by a rise in tan δ toward a (not reached) second peak. Dynamic viscoelastometry on the optically clear, inhomogeneous blends of copolymers J and K with PPO resin has not yet been done.

Conclusions

Statistical copolymers of styrene–*p*-chlorostyrene (M_w ~3 –4 × 10^5) having cumulative mole fraction styrene $\bar{N}_s \geq 0.347$ form homogeneous, single-phase blends with PPO resin (M_w = 3.72 × 10^4). Styrene–*p*-chlorostyrene copolymers having cumulative $\bar{N}_s \leq 0.320$ form heterogeneous blends with PPO resin. A copolymer having cumulative $\bar{N}_s$ = 0.334 also appears incompatible with PPO resin, but it is definitely a borderline case. In the five blend systems for which thermo-optical, differential scanning calorimetric, and dynamic viscoelastic data were all obtained, each distinguished the homogeneous or heterogeneous character of the blends examined by detecting respectively one or two transition temperatures. The detection methods applied, and the results observed, are indicated in Table II. The relative sensitivities of these analytical tests for mobility transitions in detecting single or multiple glass transitions require further examination. Blends of copolymers K, J, M, and N with PPO resin should serve well for such future studies.

An attempt to assess the variation of copolymer–PPO resin thermodynamic interaction parameters with copolymer composition will be made in a forthcoming paper in which copolymer average molecular weights are varied.

References and Notes

(1) (a) Paper presented at the 6th Biennial Polymer Symposium, University of Michigan, Ann Arbor, Mich., June 12–15, 1972; (b) registered trademark of the General Electric Co.
(2) J. Stoelting, F. E. Karasz, and W. J. McKnight, *Polym. Sci. Eng.*, **10**, 133 (1970).
(3) (a) H. E. Bair, *Polym. Sci. Eng.*, **10**, 247 (1970); (b) A. R. Shultz and B. M. Gendron, *J. Appl. Polym. Sci.*, **16**, 461 (1972).
(4) J. Heijboer, *Plastica*, **19**, 489 (1966).
(5) J. Heijboer, *J. Polym. Sci., Part C*, **16**, 3755 (1968).
(6) S. dePetris, V. Frosini, E. Butta, and M. Baccaredda, *Makromol. Chem.*, **109**, 54 (1967).
(7) F. E. Karasz, J. M. O'Reilly, H. E. Bair, and R. A. Kluge, *Polym. Prepr., Amer. Chem. Soc., Div. Polym. Chem.*, **9**, 822 (1968).
(8) F. E. Karasz, H. E. Bair, and J. M. O'Reilly, *J. Polym. Sci., Part A-2*, **6**, 1141 (1968).
(9) G. Allen, M. W. Coville, R. M. John, and R. F. Warren, *Polymer*, **11**, 492 (1970).
(10) R. Simha and L. A. Wall, "Styrene. Its Polymers, Copolymers, and Derivatives," R. H. Boundy and R. F. Boyer, Ed., Reinhold, New York, N. Y., 1952, Chapter 20.
(11) F. M. Lewis, C. Walling, W. Cummings, E. R. Briggs, and F. R. Mayo, *J. Amer. Chem. Soc.*, **70**, 1519 (1948).

Low Temperature Thermal Expansions and Relaxations in Polyethylene

Shirley Lee and Robert Simha*

Department of Macromolecular Science, Case Western Reserve University, Cleveland, Ohio 44106.

Received June 24, 1974

ABSTRACT: Thermal expansivities α for two linear and a branched polyethylene have been measured between 100°K and room temperature. Both α and the derivative $d\alpha/dT$ are reported as a function of temperature and the results compared with low frequency dynamic data. In the region corresponding to the dynamically observed γ loss, two distinct dilatometric relaxations are found in all three polymers. The results are compared with those obtained previously for Nylons 66 and 11. Similarities and differences in the γ region are discussed in terms of various local motions proposed. Two additional relaxation regions are detectable at about 180 to 195°K. Above *ca.* 200°K, only a steep rise in α is discernible for both linear species, whereas the branched polymer exhibits stepwise increments.

In recent years we have extensively investigated the thermal expansivities of polymers at low temperatures in the amorphous[1] and in the semicrystalline state.[2] Accurate dilatometry has been demonstrated to be a successful low frequency method in dynamic mechanical investigations and, by virtue of the low effective frequency (10^{-3}–10^{-4} Hz), to resolve adjacent relaxation regions, where other methods may not indicate more than a shoulder in the plot of loss modulus *vs.* temperature.[1]

In this context polyethylenes are of particular interest, due to their simple structure, relatively high cyrstallinity, and the resulting controversies in the interpretation of their relaxation spectra. Thermal expansivities of a low density polyethylene and its copolymers with propylene have been reported.[2a] Volumes or lengths as a function of temperature have been measured by several authors.[3-5] They either give the volume–temperature results or their derivatives, using large temperature intervals. This makes it difficult at best to detect possible fine structures in the relaxation spectrum.

The purpose of this paper is to present dilatometric results for two linear and a branched polyethylene in the temperature range of 100–300°K, comparisons with two nylons, and tentative interpretations. Instrumentation and procedures have been previously described.[1c]

I. Materials and Experimental

The National Bureau of Standards' linear polyethylene (LPE), SRM 1475, and branched polyethylene (BPE), SRM 1476, were employed. To these was added the high molecular weight linear polymer (HMLPE), manufactured by and obtained from Allied Chemical Co. Characteristics of the three polymers are summarized in Table I. The melting points were determined by Olabisi.[6] Samples were compression molded into thin sheets (15–25 mils) at 30°K above their respective T_m's. Strips of 1.5 in. × 0.5 in. × 0.02 in. were cut from the molded sheet and then mounted on the double Dewar dilatometer. Cooling from room temperature to *ca.* 100°K was accomplished by filling the outer Dewar with liquid nitrogen. The inner one was filled with helium gas to promote heat transfer. The temperature of the copper block where the specimen resides was gradually raised at a constant heating rate of 0.5°/min. Length and temperature readings were recorded at 1° intervals. Linear